Deterministic side-branching during thermal dendritic growth

Deterministic side-branching during thermal dendritic growth

Andrew M Mullis[1a]

[1]Institute for Materials Research, University of Leeds, Leeds LS2-9JT, UK.

E-mail: [a] a.m.mullis@leeds.ac.uk

Abstract. The accepted view on dendritic side-branching is that side-branches grow as the result of selective amplification of thermal noise and that in the absence of such noise dendrites would grow without the development of side-arms. However, recently there has been renewed speculation about dendrites displaying deterministic side-branching [see e.g. ME Glicksman, Metall. Mater. Trans A 43 (2012) 391]. Generally, numerical models of dendritic growth, such as phase-field simulation, have tended to display behaviour which is commensurate with the former view, in that simulated dendrites do not develop side-branches unless noise is introduced into the simulation. However, here we present simulations at high undercooling that show that under certain conditions deterministic side-branching may occur. We use a model formulated in the thin interface limit and a range of advanced numerical techniques to minimise the numerical noise introduced into the solution, including a multigrid solver. Not only are multigrid solvers one of the most efficient means of inverting the large, but sparse, system of equations that results from implicit time-stepping, they are also very effective at smoothing noise at all wavelengths. This is in contrast to most Jacobi or Gauss-Seidel iterative schemes which are effective at removing noise with wavelengths comparable to the mesh size but tend to leave noise at longer wavelengths largely undamped. From an analysis of the tangential thermal gradients on the solid-liquid interface the mechanism for side-branching appears to be consistent with the deterministic model proposed by Glicksman.

1. Introduction

One of the most fundamental and all pervasive microstructures produced during the solidification of metals is the dendrite. The dendrite is a prime example of a pattern forming system where complex morphologies arise from initially homogeneous conditions due to the highly non-linear response of the controlling system. The formation of the secondary (and higher order) side-branches has been an area of particular interest as it is these secondary arms that give dendrites their characteristic morphology.

Imaging of dendritic growth in transparent analogue casting systems, such as succinonitrile [1] and xenon [2], show that close to the tip region the dendrite is apparently free from side-branching. Moving away from the tip small oscillations are initiated which grow as they move down the dendrite trunk. Initially the spacing of these perturbations is uniform. However, as amplification of the initial perturbations proceeds the process becomes competitive with faster growing side-arms becoming dominant, leading to a less uniform spacing. Eventually coarsening becomes dominant, with side-arms of higher curvature being preferentially re-melted [3, 4].

A number of measures have been proposed to quantify the side-branch morphology of dendritic structures. The simplest, and often the only measure that can be applied to as-solidified materials, is the secondary arm spacing, λ_2. However, when the growing dendrite can be imaged *in situ* a far greater range of measures may be applied. The most direct is $\bar{z}_{sb}$, which is the mean distance along

the trunk (in units of ρ) at which the amplitude of the side-branching becomes equal to ρ, ρ being the radius of curvature at the dendrite tip. Other measures which have been used in the literature [2, 5] to characterise dendritic structures include the fractal dimension, shape parameterization of the inner and outer side-branch envelopes, projection area and contour length.

Probably the most carefully controlled study of dendritic growth to be undertaken is the Isothermal Dendrite Growth Experiment [6] (IDGE), in which the onset of side-branching, as measured by the distance to the first detectable side-branch, was determined for high purity succinonitrile under microgravity conditions. This was determined as being at $(11.8 \pm 1.7)\rho$. In a control experiment, which was identical except that it was performed under terrestrial gravity, the same measurement yielded $(12.7 \pm 2.3)\rho$. Bisang & Bilgram [2] have measured $\bar{z}_{sb}$ for xenon dendrites under terrestrial conditions, finding $\bar{z}_{sb} = (17.5 \pm 3)\rho$. This figure is somewhat higher than that found during IDGE due to the different methodologies applied, the first detectable side-branch having an amplitude significantly less than ρ, so that the two data sets are probably mutually consistent.

The generally accepted theory of side-branch formation during dendritic growth is that side-branches grow due to the selective amplification of thermally induced noise at the solid-liquid interface with models for this process, in the framework of microscopic solvability theory, having been put forward by Langer [7, 8] and by Brener & Tempkin [9]. Such models appear to be supported by a number of phase-field simulations, in which it has been observed that dendrites grow without side-branches unless noise is introduced at the solid-liquid interface [10], with the observed level of side-branching increasing both with the strength of the noise and the undercooling (or equivalently, velocity) at which the dendrite grows [11]. Recently however, based upon a re-evaluation of the IDGE data, Glicksman [12, 13] has proposed that dendrites may undergo deterministic side-branching. The proposition is that capillary mediated differences in the temperature of the solid-liquid interface give rise to heat currents (termed bias-fields) which lead to the onset side-branching even in the absence on thermally induced noise. It is argued in [12, 13] that although the temperature difference along the solid-liquid interface in minute, due to the small length scales involved the thermal gradient may not be. It has also been pointed out [14] that if an anisotropic capillary mediated temperature distribution is calculated for a *parabolic* dendrite, a temperature inversion will arise near the tip for anisotropies exceeding 0.011, that is the lowest temperature is attained not at the tip but at some point downstream of the tip. Moreover, even if the interface temperature decreases monotonically moving back from the dendrite tip, due to the curvature of the interface the tangential thermal gradient is not unidirectional. It is argued that the point on the interface at which the gradient reverses is the point of initiation of deterministic side-branching as here there is an inward heat flow from both the dendrite tip and the downstream region which therefore perturbs the dendrite shape.

Contrary to most phase-field studies, Wang et al. [15] did find evidence of side-branching in the absence of artificially introduced noise for dendrites grown at the high undercooling of $\theta_{sys} = 0.8$, apparently in support of the ideas proposed by [12, 13]. Here θ_{sys} is the dimensionless bulk undercooling, $\theta_{sys} = H\Delta T/C_p$, H being the latent heat on fusion and C_p the specific heat. However, such investigations are potentially fraught with pit-falls. In particular, unless considerable care is taken it is difficult to ensure that the numerical noise is not introduced into the solution via the computational scheme employed. This is particularly the case when explicit solution schemes of the forward Euler type are used with a fixed (stability limited) time-step at high undercooling, wherein the dendrite grows further per time-step, potentially introducing noise which may initiate side-branching.

In this paper we re-evaluate the findings of [15], using a thermal phase-field model formulated using a range of advanced numerical techniques designed to minimise the noise introduced in to the solution by the numerical scheme. In particular, we use an implicit time-stepping scheme with a non-linear multigrid solver which is a particularly efficient way of obtaining low noise solutions to a set of coupled partial differential equations. Typically, a Jacobi or Gauss-Seidel iteration is efficient at smoothing noise at wavelengths comparable to the mesh spacing, h, but very inefficient at smoothing noise at longer wavelengths, which therefore tends to remain in the solution. In multigrid, the

restriction of the solution to progressively coarser nested meshes means that noise at all wavelengths is efficiently smoothed. Moreover, the time-step in the implicit solution is limited by the accuracy of the solution, not its stability. Therefore, by employing a dynamically adjusting variable time-step determined by a series of error estimators based upon the norm of the residuals in the solution we can ensure that the same level of accuracy is obtained in all solutions irrespective of the growth rate.

2. Computational Model

The model adopted here is based upon that of [16] in which, following non-dimensionalization against characteristic length and time scales, W_0 and τ_0, the evolution of the phase-field, ϕ, and the dimensionless temperature field, θ, are given by

$$A^2(\psi)\frac{\partial \phi}{\partial t} = \nabla \cdot \left(A^2(\psi)\nabla \phi\right) + \phi(1-\phi^2) - \lambda\theta(1-\phi^2)^2$$

$$-\frac{\partial}{\partial x}\left(A(\psi)A'(\psi)\frac{\partial \phi}{\partial y}\right) + \frac{\partial}{\partial y}\left(A(\psi)A'(\psi)\frac{\partial \phi}{\partial x}\right) \qquad (1)$$

$$\frac{\partial \theta}{\partial t} = \alpha\nabla^2\theta + \frac{1}{2}\frac{\partial \phi}{\partial t} \qquad (2)$$

where, for 4-fold growth, $A(\psi) = 1 + \varepsilon.\cos(4\psi)$, d_0 is the chemical capillary length, k_E is the equilibrium partition coefficient, α is the dimensionless thermal diffusivity and λ is a coupling parameter given by $\lambda = \alpha/a_2 = a_1 W_0/d_0$ with a_1 and a_2 taking the values $5\sqrt{2}/8$ and 0.6267 respectively [17].

The governing equations are discretized using a finite difference approximation based upon a quadrilateral, non-uniform, locally-refined mesh with equal grid spacing in both directions. Second differentials are calculated using a (spatially) forth order accurate 9-point stencil, while a compact 17-point forth order stencil has been used for Laplacian terms, in order to reduce the mesh induced [18] anisotropy. The stencils, and the weights associated with each point therein, are illustrated graphically in Fig. 1. To ensure sufficient mesh resolution around the interface region local mesh refinement (coarsening) is employed when the weighted sum of the gradients of ϕ and θ exceeds (falls below) some predefined value.
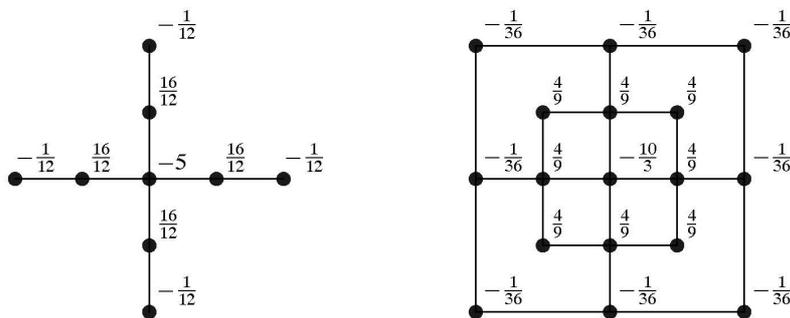

Figure 1. 9 and 17-point finite difference stencils used to evaluate the second differentials and Laplacian terms in Equations (1-2).

An implicit temporal discretization is employed based on the second order Backward Difference Formula with variable time-step, wherein it is necessary to solve a very large, but sparse, system of non-linear algebraic equations at each time-step. Multigrid methods are among the fastest available solvers for such systems and in this work we apply the non-linear generalization known as FAS (full approximation scheme [19]). The local adaptivity is accommodated via the multilevel algorithm originally proposed by Brandt [20]. The interpolation operator is bilinear while injection is used for

the restriction operator.   For smoothing the error we use a fully-coupled nonlinear weighted Gauss-Seidel iteration where the number of pre- and post-smoothing operations required for optimal convergence is determined empirically. Full details of the numerical scheme are given in [21].

3. Numerical Results

Figure 2 compares the morphology of the solid liquid interface for dendrites grown at θ_{sys} = 0.6875 and θ_{sys} = 0.8000, the other computational parameters for these simulations being α = 1, ε = 0.03 and h = 0.78. The domain size, Ω, is $[-1600:1600]^2$ and the initial seed with radius 5 is located at the centre of the domain. It is apparent that from the plots that spontaneous side-branching is occurring at high undercooling but not at lower undercooling. While superficially these results look like those of [15] there are two important differences. Firstly, although [15] present images (e.g. their Figs. 2a and 3a) showing equiaxed dendrites with 4-fold symmetry, their simulations are in fact conducted on a quarter domain with the equiaxed dendrite being created by rotating and replicating a single primary branch. In contrast, the equiaxed dendrite shown in this work (Fig. 2b) is nucleated from a seed in the middle of the domain. Each of the primary arms shown has therefore grown independently and the fact that each shows an identical branching pattern in itself represents strong evidence of a deterministic branching mechanism as numerical noise, by its random nature, would give rise to different patterns on each primary branch. Secondly, in [15] very low anisotropies are used in order to obtain branching. Strong branching is evident at ε = 0.005, with branching becoming almost indiscernible at ε = 0.02. It is well known that noise induced side-branching is suppressed by strong capillary anisotropy. In contrast the branched dendrite shown in Fig. 2b is grown at the relatively high anisotropy of ε = 0.03. In deed, if we very the anisotropy and determine the dimensionless undercooling, θ_{sys}, required for the onset of spontaneous side-branching we find that θ_{sys} decreases as ε increases, as shown in Fig. 3. This suggests that the mechanism responsible is not the same as operating in the simulations reported by [15] and is not related to the amplification of numerical noise.
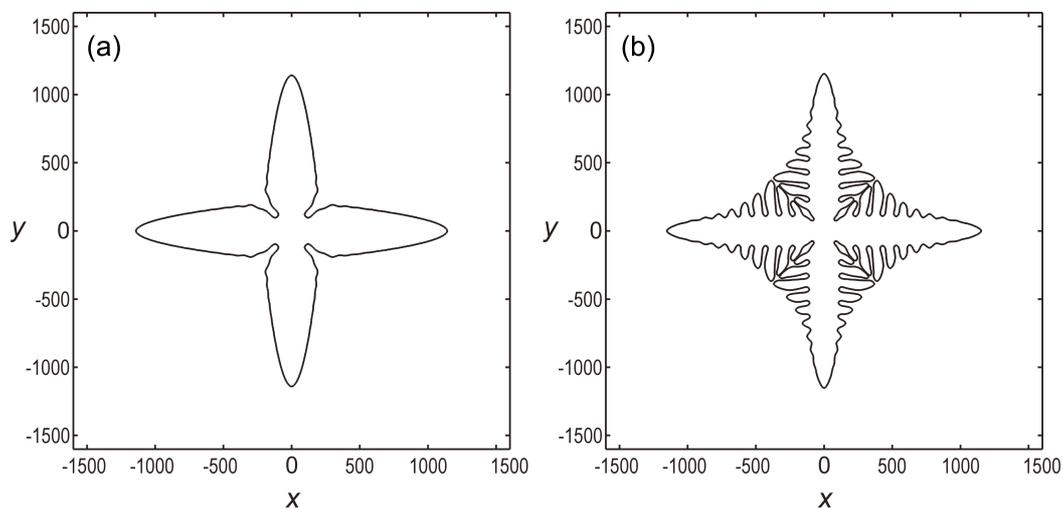

Figure 2. Example phase-field dendrite morphologies at a system undercooling of (a) θ_{sys} = 0.6875, without side-branching and (b) θ_{sys} = 0.8000, displaying spontaneous side branching.

To investigate the mechanism for side-branch formation in these simulated dendrites and to explore the similarities with the deterministic side-branching mechanism proposed in [12, 13] it is instructive to look in some detail at the temperature distribution at the dendrite tip. Figure 4 compares (a) the temperature distribution obtained when an anisotropic surface energy is imposed upon an exactly parabolic needle crystal with (b) the temperature distribution obtained from a phase-field dendrite (b).

In both cases $\varepsilon = 0.03$ and in the phase-field simulation $\theta_{sys} = 0.6875$. The temperature distribution for the parabolic needle was obtained by (i) generating an exact parabola; (ii) calculating its curvature and hence the temperature at its interface; (iii) bringing the shape into thermal equilibrium, treating the temperature calculated in (ii) above as a Dirichlet boundary condition on the solid-liquid interface. It can be observed that in the case of the exactly parabolic needle there is indeed a temperature inversion, with the lowest temperature occurring either side of the tip. In contrast, for the phase-field dendrite no such temperature inversion is observed, with the tip being the region with the lowest temperature. In deed, in no phase-field simulation, irrespective of the undercooling at which the dendrite is grown or the anisotropy imposed upon the system, have we observed a temperature inversion on the solid-liquid interface, with the tip region always being the region lowest temperature.
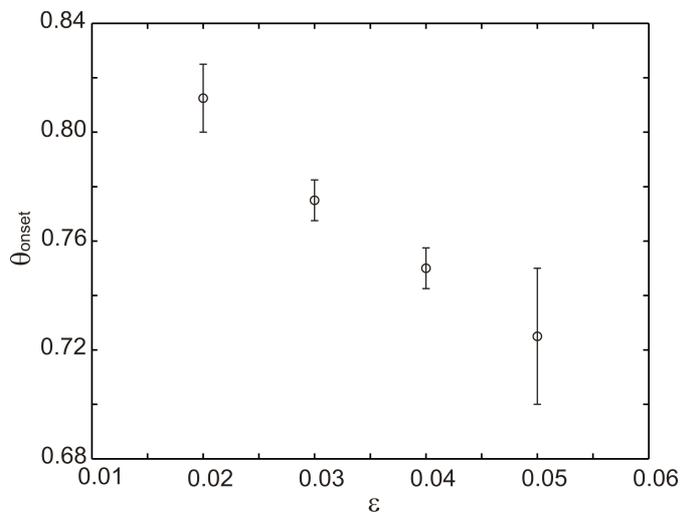

Figure 3. The undercooling, θ_{onset}, at which spontaneous side-branching is first observed as a function of the imposed anisotropy, ε.
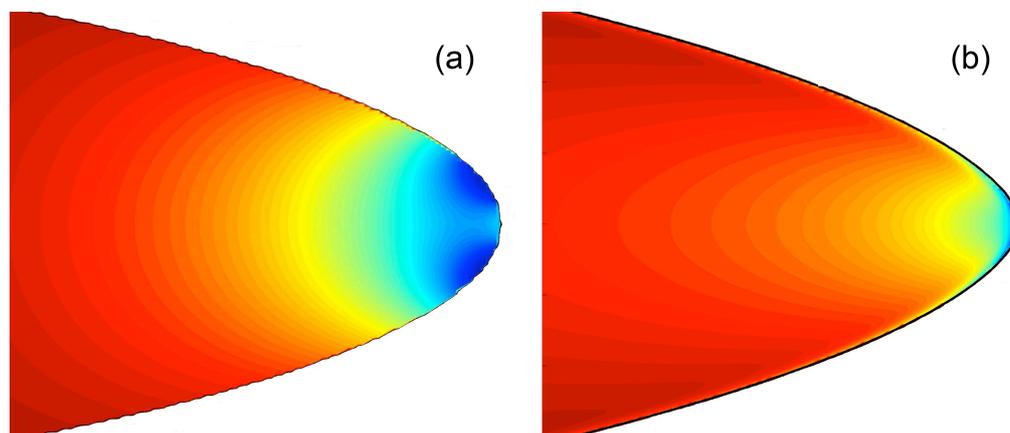

Figure 4. Thermal profile in the tip region of (a) an exactly parabolic dendrite with an anisotropic surface energy ($\varepsilon = 0.03$) and (b) a phase-field dendrite growing with a surface energy anisotropy of $\varepsilon = 0.03$.

This appears to be because the shape of the dendrite tip alters in response to the imposed anisotropy in such a way that a temperature inversion is avoided. Specifically, as the anisotropy is increased the curvature increases more rapidly as one approaches the tip than would be the case for the equivalent parabolic crystal. This can be seen most readily by calculating the actual and parabolic radii

of curvature, ρ_a and ρ_{para} respectively, for the phase-field dendrites. Here, if (X, Y) is the locus of the solid-liquid interface (the $\phi = 0$ isoline), ρ_a is given, for a dendrite growing along the x-direction, by

$$K = \frac{\partial^2 X / \partial Y^2}{\left(1 + \left(\partial X / \partial Y\right)^2\right)^{3/2}} \ , \quad \rho_a = \frac{1}{|K|} \tag{3}$$

The parabolic tip radius is given by fitting a curve of the form

$$Y^2 = -2\rho_{para}(X - X_0) \tag{4}$$

to the down-stream region of the dendrite, typically the region $2\rho_a$ behind the tip. The procedure for calculating ρ_{para} is given in more detail in [16]. In Figure 5 we plot the ratio ρ_{para}/ρ_a as a function of system undercooling and anisotropy. It can be seen that the ratio ρ_{para}/ρ_a increases rapidly with increasing ε while there is a much smaller variation as a function of undercooling, i.e. that as the anisotropy increases the tip region sharpens more rapidly than would be expected from the near parabolic down-stream shape, thus avoiding a temperature inversion at the tip.
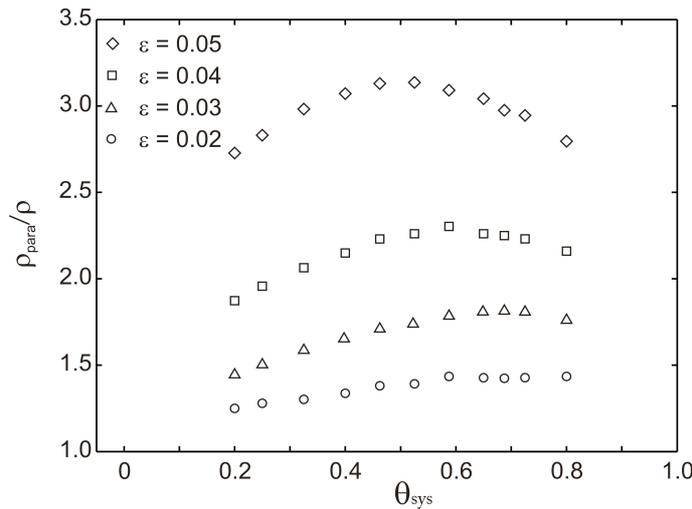

Figure 5. Ratio of the parabolic to the actual tip radius as a function of undercooling and anisotropy. As the anisotropy increases the tip becomes progressively sharper, relative to the down-stream parabolic profile, with the effect that a temperature inversion at the tip is avoided.

However, as pointed out in [12, 13], due to the curvature of the solid liquid interface the tangential thermal gradient evaluated on the interface may not be monotonic, even if the temperature does decrease monotonically moving down-stream from the tip. For the phase-field model this tangential surface thermal gradient may be evaluated from

$$\hat{\Phi} = \frac{\phi_x \theta_y - \phi_y \theta_x}{|\nabla \phi|^2} \tag{5}$$

where the subscripts denote differentiation with respect to x or y respectively. A plot of $\hat{\Phi}$ as a function of the distance downstream from the dendrite tip is shown in Fig. 6, for the dendrite displaying side-branching in Fig. 2b. The similarity in the form of the curve shown in Fig. 6, calculated for a phase-field dendrite, with the profiles calculated analytically by Glicksman [see e.g. Fig. 5 in Ref. 12] is remarkable. In particular, in both cases the curve has a turning point somewhat downstream from the tip and it is this turning point in the tangential thermal gradient which [12, 13] has associated with the deterministic side-branching mechanism. Note that the co-ordinate system

used here is different from that in [12, 13] in which an elliptic geometry was considered. Here, the phase-field simulation results in the growth of a near parabolic dendritic crystal. The abscissa on Figure 5 is therefore the distance back from the dendrite tip expressed in units of the actual tip radius, ρ_a. For reference this tip radius is $\rho_a = 6.55$.
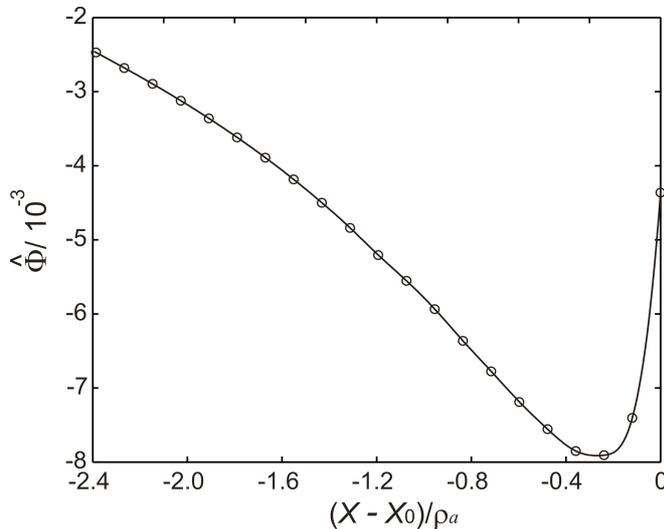

Figure 6. The tangential thermal gradient calculated on the solid-liquid interface for a dendrite with $\theta_{sys} = 0.8$ and which is displaying spontaneous side-branching.

One of the distinguishing features in Fig. 6 is that the turning point in $\hat{\Phi}$ is very close to the tip at $X - X_0 = 0.3\rho_a$. In contrast the first detectable side branch is at $X - X_0 = -28\rho_a$. In order to determine whether the tangential thermal gradients shown in Fig. 6 might potentially be perturbing the dendrite shape very close to the tip and thereby having an effect leading to observable side branching further downstream the following procedure has been adopted. The tip region of the dendrite (from $X - X_0 = 0$ to $X - X_0 = -15\rho_a$) has been fitted with an order n polynomial, where n is 4-5. This is of sufficiently high order to capture the non-parabolic tip shape but not of sufficiently high order to capture perturbations to the tip-shape from side-branching. We have then calculated the residuals between the fit and the original data to identify small perturbations to the dendrite shape. The results of this analysis, $\theta_{sys} = 0.8000$, are shown in Fig. 7, wherein it can be seen that there is indeed a cyclic perturbation to the dendrite tip shape. Moreover, the initial perturbation is located at $X - X_0 = -0.3\rho_a$, co-incident with the minimum in the tangential thermal gradient shown in Fig. 6. We take this to be at least suggestive that the heat flow associated with the tangential surface gradients and the observed side-branching are causally related. We also note that the period of the perturbations in Fig. 7 ($\sim 7.4\rho_a$), is almost exactly half the period of the finally observed side-branching, the mean secondary dendrite arm spacing being $14.7\rho_a$. As an aside we note (not shown due to reasons of brevity) that at lower undercoolings the calculated tangential thermal gradient has a similar form to that shown in Fig. 6, but that the magnitude of the minimum decreases as the undercooling is decreased. This still appears to lead to the occurrence of a shape perturbation within $-3\rho_a \leq X - X_0 \leq -0.1\rho_a$ of the tip. However, unlike the perturbations shown in Fig. 7, as we move downstream from the tip the amplitude of the perturbation is decreasing, rather than increasing. This suggests that there is an amplification condition that needs to be satisfied before deterministic side-branching will be manifest.

5. Conclusions
By using a phase-field model incorporating a range of advanced numerical techniques designed to achieve high solution accuracy with minimal induced numerical noise we have been able to demonstrate that under certain circumstances dendrites may undergo spontaneous, deterministic side-branching. Calculation of the tangential thermal gradients on the phase-field solid-liquid interface and comparison of these with location of the first perturbation on the solid-liquid interface appear to be

consistent with the capillary mediated 'bias-field' branching mechanism proposed by Glicksman [12, 13]. However, the occurrence of such side-branching appears to be confined to high undercooling/growth velocity. At low velocity the amplitude of the perturbations decreases downstream, eventually decaying away. The mechanism for this is not yet fully understood.
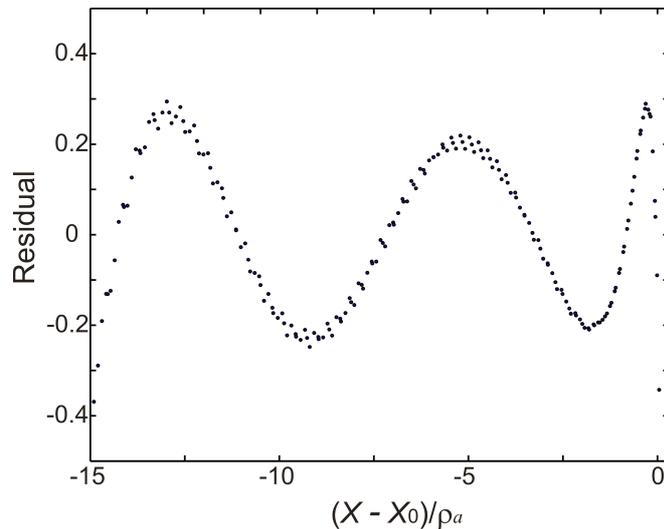

Figure 7. Residual between the actual shape of a phase-field dendrite grown at $\theta_{sys} = 0.8$ and an order 4 polynomial fit to the tip region. This procedure is very efficient at showing up small cyclic perturbations to the tip region. Note that the perturbations begin near $X-X_0 = -4d_0$, which is the location of the minimum in $\hat{\Phi}$

6. References

[1]   Corrigan D P, Koss M B, La Combe J C, DeJager K D, Tennenhouse L A and Glicksman M E 1999 *Phys. Rev. E* **60** 7217.
[2]   Bisang U and Bilgram J H 1996 *Phys. Rev. E* **54** 5309.
[3]   Kattamis T Z, Coughin J C and Flemings M C 1967 *Trans. Met. Soc. AIME* **239** 1504.
[4]   Young K P and Kirkwood D H 1975 *Met. Trans.* **6A** 197.
[5]   Li Q and Beckermann C 1998 *Phys. Rev. E* **57** 3176.
[6]   Tennerhouse L A, Koss M B, LaCombe J C and Glicksman M E 1997 *J. Cryst. Growth* **174** 82.
[7]   Barber M N, Barbieri A and Langer J S 1987 *Phys Rev. A* **36** 3340.
[8]   Langer J S 1987 *Phys. Rev. A* **36** 3350.
[9]   Brener E and Temkin D 1995 *Phys. Rev. E* **51** 351.
[10]   Warren J A and Boettinger W J 1995 *Acta metall. mater.* **43** 689.
[11]   Mullis A M 2001 *Acta mater.* **49** 2205.
[12]   Glicksman ME 2012 Coherent Capillary-mediated dendritic branching *Proc. MCWASP XIII (Schladming, Austria, 17–22 June 2012) IOP Conf. Series: Materials Science and Engineering* **33** 012097.
[13]   Glicksman ME 2012 *Metall. Mater. Trans.* **43A** 391.
[14]   Glicksman ME 2012 Oral presentation at *MCWASP XIII (Schladming, Austria, 17–22 June 2012)*.
[15]   Wang Z, Wang J and Yang G 2008 *Phys. Rev. E* **78** 042601.
[16]   Rosam J, Jimack P K and Mullis A M 2008 *Acta Mater.* **56** 4559.
[17]   Karma A 2001 *Phys. Rev. Lett.* **87** 115701.
[18]   Mullis A M 2006 *Comp. Mater. Sci.* **36** 345.
[19]   Trottenberg U, Oosterlee C and Schuller A 2001 *Multigrid* (Academic Press, London).
[20]   Brandt A 1977 *Math. Comp.* **31** 333.
[21]   Rosam J, Jimack P K and Mullis A M 2007 *J. Comp. Phys.* **225** 1271.